JOURNAL OF MATERIALS SCIENCE 12 (1977) 857–868

Review
Metallurgical applications of scanning transmission electron microscopy

K. E. EASTERLING
Department of Materials Technology, University of Luleå, S-951 87 Luleå, Sweden

It is shown that scanning transmission electron microscopy (STEM) has followed two main lines of development, the pure STEM based upon a field emission electron source in which the emphasis is given to high resolution, and a combined system in which STEM is an attachment to a conventional transmission microscope (TEM + STEM). When used in combination with an energy dispersive X-ray spectrometer, the combined TEM + STEM system is shown to be extremely versatile and possibly the more useful for the applied metallurgist. The high vacuum requirements of pure STEM, however, make this system suitable to be used in conjunction with an Auger spectrometer. Examples of the various microanalysis facilities of STEM are given in the article, including micro-diffraction, rocking-beam channelling patterns, qualitative and quantitative X-ray spectroscopy analysis, particle analysis and *in situ* experimentation. The controversial subject of whether thicker specimens can be studied in STEM compared with conventional TEM is also discussed.

1. Introduction

Over the last couple of decades, electron microscopy has grown to be the most important tool of the physical metallurgists' trade. By the mid-sixties transmission microscopy had already made substantial contributions towards metallurgists' understanding of the nature and defect structure of metals and alloys, had brought precision and sophistication to their craft, and had helped them to substantiate the foundations of their science. The introduction later of scanning electron microscopy with its associated chemical analysis facilities widened the metallurgists' scope and brought them into closer contact with engineers and the applied technologies. From the instrumentation point of view, of course, scanning microscopy also marked a new era in electron optics, opening up many new ways of image processing and formation. Indeed, in many respects scanning microscopy proved to be more versatile than transmission microscopy and the technique was rapidly established in both university and industrial laboratories throughout the world as an important technologically oriented instrument. Its drawback of course, was the fact that it was limited to surface observations, and with high voltage (1000 kV) transmission microscopy beginning to excite the interest of physical metallurgists in the late sixties it seemed for a time that the two important techniques of transmission and scanning microscopy would continue to pursue their own separate paths of development.

It was left to Crewe and his co-workers [1–5] working at the University of Chicago on a new scanning microscope fitted with a field emission source, to demonstrate the many advantages of transmitted image formation. It was found that by placing an electron detector below a thin sample in a scanning microscope, information of the internal structure of materials could be obtained and processed in a similar way to which the reflected

electrons from surfaces were already being processed in conventional scanning microscopy. Ironically, the first scanning electron microscope built by Ardenne in 1938 also incorporated the detector *below* a thin sample. The two important techniques of scanning and transmission electron microscopy were thus brought firmly together and the new technique of scanning-transmission electron microscopy (STEM) was (re)established.

In recent years STEM has developed along two distinct lines and within the last 2 to 3 years it has been commercially available either as an attachment to a conventional transmission microscope (TEM + STEM), or as a "pure" STEM based on a field emission gun. The four alternatives of conventional TEM, conventional SEM, TEM + STEM and pure STEM are compared in Table I in terms of their various uses and possible applications. It is seen that not only does STEM retain the main advantages of both conventional TEM and SEM, it also generates several new analytical possibilities such as micro-diffraction and high resolution thin foil chemical and image analysis. Even the technique's resolution in scanning mode is better than that of conventional SEM because of the higher brightness gun and better lens system used. As indicated by Table I, the TEM + STEM alternative is probably the more useful to metallurgists at present, and is the most suitable for X-ray spectroscopy chemical analysis. On the other hand, the high vacuum requirements of the field emission pure STEM may open up possibilities for combined Auger spectroscopy in conjunction with high resolution structural observation.

Practical experience with scanning transmission electron microscopy has been very limited to date and the purpose of this article is to review initial work in an attempt to see how the technique with its associated attachments is likely to be useful to metallurgists in the near future.

2. Principles of scanning transmission electron microscopy

The electron optics of scanning transmission electron microscopy are illustrated schematically in Fig. 1. In contrast to the essentially parallel beam employed in conventional transmission microscopy, in stem the beam is focused to a fine probe and scanned over the samples as in

TABLE I Comparison of the various electron microscope techniques commercially available, illustrating their respective versality and usefulness (data mostly from manufacturers' brochures, news sheets, etc)

Available technique	Conventional (100 kV) TEM	Conventional SEM (30–50 kV)	Pure STEM (100 kV) (field emission gun)	(TEM + STEM) 100–200 kV thermionic W filament gun
Transmission microscopy	Yes; res. ~0.001 μm	No	No	Yes, res. ~0.001 μm
Electron diffraction	Yes. res. ~1 μm	No	No	Yes, res. ~1 μm
Scanning microscopy	No	Yes, res. ~0.01 μm	Yes, res. ~0.002 μm	Yes, res. ~0.005 μm
Scanning transmission microscopy	No	No	Yes, res. ~0.001 μm	Yes, res. ~0.003 μm
Micro-diffraction	No	No	Yes, res. ~0.01 μm	Yes, res. ~0.02 μm
Channelling patterns	No	Yes, res. ~5–10 μm	Yes, res. ~3 μm	Yes, res. ~3 μm
Standard attachments in common use	None	EDX; res. ~1.0 μm WDX; res. ~1.0 μm *In situ* experiment stages e.g. deformation, environmental, etc.	None	EDX, res. ~0.05 μm *In situ* experiment stages
Useful possible attachments	Energy-loss spectroscopy res. ~0.01 μm	Image analyser for measuring e.g. particle size, volume fraction, second phase, etc.	Auger spectroscopy: res. <1 μm area, 0.001 μm depth. Image analysis.	Energy-loss spectroscopy Image analysis

SEM. Electrons passing through the sample are collected and processed as in conventional SEM. If other detectors are placed above the sample, the microscope can also be used as a high resolution SEM. If fitted to a conventional transmission microscope as a beam focusing and scanning attachment, the combined system can be operated either in TEM mode (retaining normal transmission and electron diffraction facilities), or in STEM mode. Besides reflected and transmitted modes of structural observation, the electron optics of STEM also make it suitable for micro-diffraction and channelling pattern modes, while the high probe current in the focused beam make it very suitable for X-ray spectroscopy.

The resolution of STEM is effectively determined by the probe size used. The size of probe (d) obtained is controlled by such factors as the gun brightness (β), the current in the probe at the specimen (I) and the beam convergence (2α). The relationship between the probe size and these various parameters is given by the expression:

$$d = (4I/\beta\pi^2\alpha^2)^{1/3}. \quad (1)$$

Probe sizes in STEM can be estimated from the sharpness of high contrast edges of features in micrographs. These estimations give a resolution in 100 to 200 kV TEM + STEM systems based on tungsten thermionic filament guns of ~0.003 μm in transmission mode and better than ~0.005 μm in SEM mode [6–8] and of ~0.0003 μm when based on the brighter field emission emitters [10]. The theoretically determined relationship between probe diameter and probe current as a function of type of emitter used [11] is illustrated in Fig. 2. It is seen that while very small probe sizes and hence high resolutions can be obtained by using the field emission source, this emitter may be limited to comparatively low probe currents which makes it relatively unsuitable for X-ray work. The tungsten and boride emitters on the other hand can be used over a wider range of probe currents, with the higher brightness boride gun providing somewhat smaller probe sizes than the tungsten. Of the three, the boride gun should provide the best all round performance with regard to both small probe size and high probe current [12].

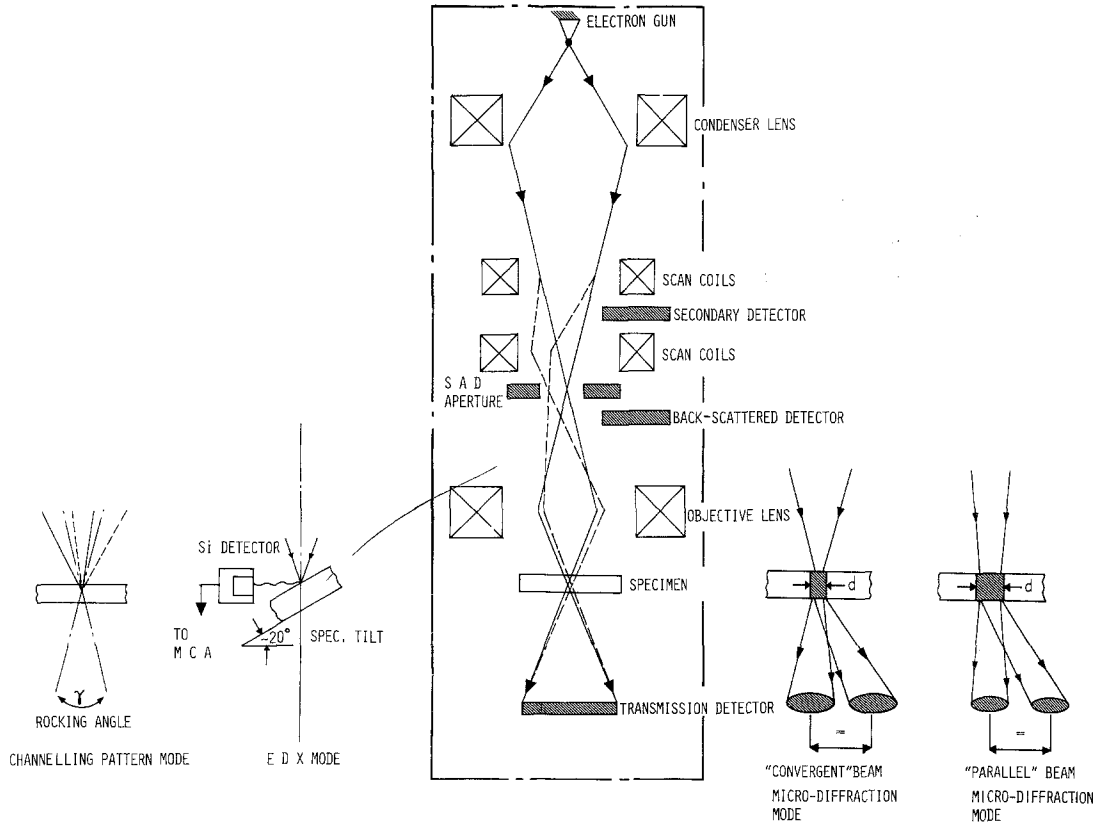

Figure 1 Schematic diagram illustrating the electron optics of scanning transmission electron microscopy and the associated techniques of channelling pattern formation, convergent and parallel beam micro-diffraction, as well as energy dispersive X-ray spectroscopy (EDX).

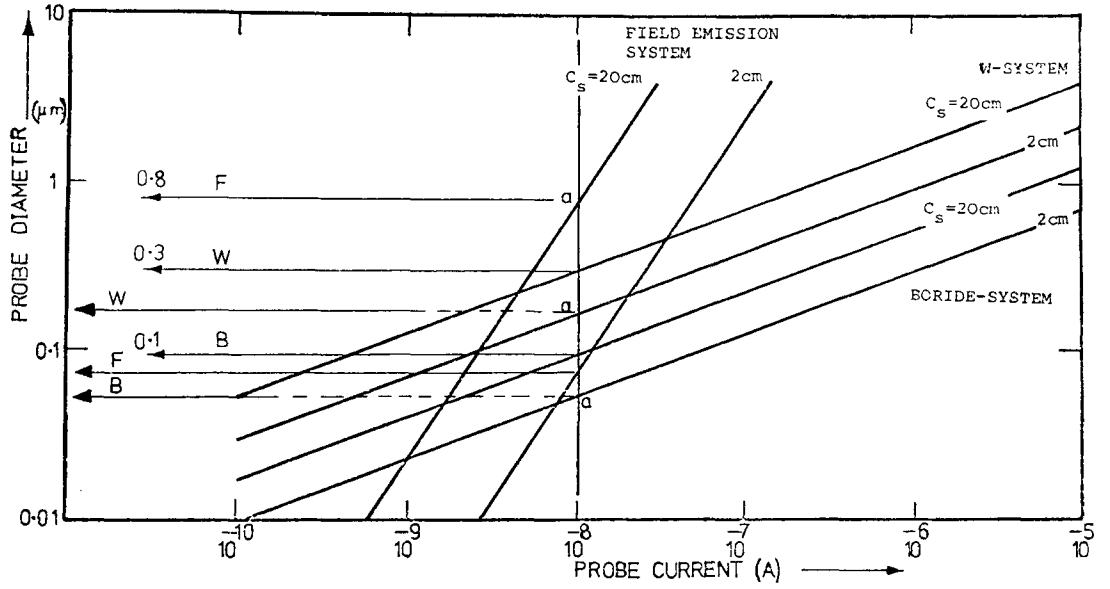

Figure 2 Log of probe diameter against log of probe current as a function of type of emitter (after Ahmed and Nixon [11]). The C_s terms refer to different values of spherical aberration.

Although prototype boride gun microscopes have been developed they suffer at present from gun instability problems. Boride guns require better vacuums than thermionic emitters, although field emission systems have the most stringent vacuum requirements of all.

Another factor affecting gun brightness is accelerating voltage. Experiments carried out in our laboratory suggest that gun brightness increases rather more than linearly with voltage. For instance the brightness estimated for a 200 kV STEM (W thermionic filament) system was $\approx 4 \times 10^9$ A m^{-2} sr^{-1}* [6] which is about five times that estimated for a 50 kV SEM. This improvement in gun brightness together with superior lens design combine to give high voltage STEMs potentially superior resolution in reflected modes over conventional SEMs. The higher brightness of STEM sources compared to conventional SEM, also allows much higher magnifications to be used on the TV monitor in SEM mode and this has proved extremely useful for *in situ* experiments on samples of ultra-fine microstructure.

Examples of the resolution obtained in transmission mode with a 200 kV TEM + STEM system are illustrated in Fig. 3a and b showing TEM and

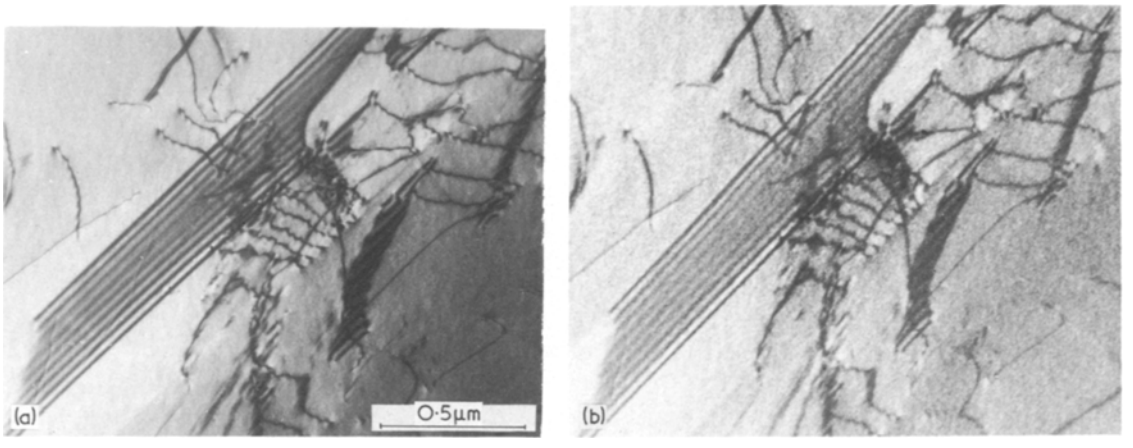

Figure 3 Comparison between (a) a 200 kV TEM image, and (b) a 200 kV STEM image of a stacking fault in stainless steel. Note that the contrast and resolution of the two images are very similar. (After Bengtsson *et al.* [6].)

*sr = steradian.

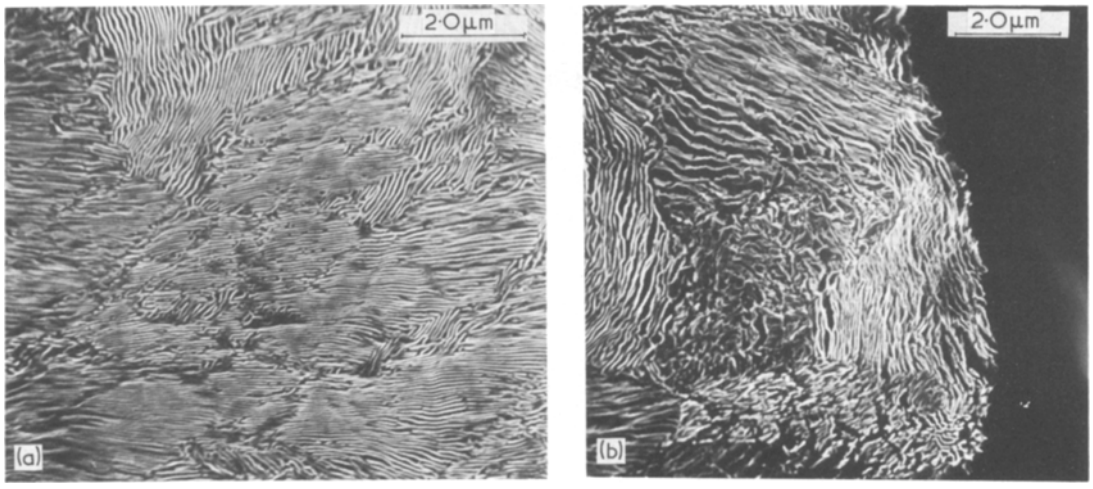

Figure 4 200 kV SEM (secondary electron back-reflected mode) micrographs of a patented steel wire under deformation in the electron microscope. TV magnifications of up to 100 000 times can be used for dynamic experiments in scanning mode which is at least ten times better than that possible with conventional scanning microscopes. Unpublished research by Smith (University of Oxford), and Bengtsson, Loberg and Easterling (University of Luleå).

STEM images of a stacking fault in stainless steel (thickness ~350 nm). Apart from a higher noise level and slightly inferior resolution in STEM mode, the two images compare well. Fig. 4a and b are 200 kV SEM micrographs from a fully pearlitic patented steel wire. This sample was tensile tested inside the microscope and TV magnifications of up to 100 000 times were routinely employed during deformation.

3. Contrast and penetration differences between STEM and TEM

As seen from Fig. 3, the contrast from STEM and TEM images appear to be very similar, and the question arises as to whether STEM image interpretation may in general be based on contrast theory already developed for conventional TEM. The similarity in contrast between STEM and TEM images derives from the fact that the electron optical geometry of stem is the reciprocal of that of TEM [5, 13, 14]. Strictly speaking, however, if operating conditions are optimized for contrast and resolution the two electron optical geometries may differ substantially. In particular, the convergence/divergence angles of the electron beam will be quite different in the two modes. In fact, the large convergence angle of the beam in STEM mode results in images that are generally less dynamic in appearance [15]. The so-called reciprocity relationship may also be affected by the different ways multiple inelastic scattering processes are sampled by the two techniques [13–15]. Furthermore, the fact that there are no image forming lenses after the objective in STEM mode implies differences in chromatic aberration which also has to be taken into account when comparing contrast between the two modes (see, however, the later discussion). On the assumption that chromatic aberration is a limiting factor when studying thick specimens in conventional TEM, STEM ought to be the better technique for studying thick samples. On this basis Seller and Cowley [16] made calculations of the improvements in contrast predicted in amorphous samples assuming equivalent electron geometries and concluded that the improvement in contrast for a given resolution, or the improvement in resolution for a given contrast could be as much as 3 or 4 in favour of STEM at 100 kV.

The little experimental work carried out to date comparing the effective electron penetration of metallic samples by the two techniques has tended to give contradictory results. Yamamoto [17] for instance found that STEM gave ~20% improvement in penetration over conventional TEM when studying a Cu–10% Al alloy, while Fraser and Jones [18] report inferior STEM penetration when studying stacking fault fringes in gold films. These authors deduced that since phonon scattering is likely to be dominant in the case of heavy elements irrespective of which technique is used, the potential advantage of STEM over TEM because of reduced chromatic aberration may only be felt when examining the light elements. In a careful study of Si, however, Fraser *et al.* [19] found that stacking fault fringe contrast deterio-

rated in STEM mode *ahead* of TEM when studying thicker sections, giving rise to the suspicion that chromatic aberration was of less importance than previously supposed [20], at least at the resolutions obtainable in STEM. On the other hand, work in our laboratory on three different metals and alloys (Al, stainless steel and W) representative of a fairly wide range of atomic number materials, showed that in all cases it was advantageous to work in STEM mode when studying very thick samples, irrespective of the material studied [6, 7]. It was found that the better image intensification available in STEM not only enabled images to be observed in thicker foils, but meant that relatively short exposure times were needed when recording the image. It is often the case that long exposure times (>1 min) cannot be tolerated due to specimen drift, and this fact proved decisive in our case.

Another good example in which the use of 200 kV STEM proved advantageous over even 1000 kV HVEM [21] is shown in Fig. 5, concerning a study of grain-boundary pores in the welding of a pressure vessel steel. In this case, the resolution is very poor, but the contrast from pores within the thick foil is at least sufficient for them to be seen.

That electron penetration in STEM mode may be superior even to high voltage microscopy is difficult to understand, and explanations of this phenomenon must await future developments in theories concerning the behaviour of transmitted electrons from fine probes. An important factor here is that the criterion adopted by Fraser *et al.* [19], involving the resolution of stacking fault fringes, is hardly realistic for many problems of metallurgical interest. If high resolution images are required, however, conventional TEM mode appears to be the most advantageous unless a field emission STEM is used.

Figure 5 STEM micrograph (X 8500) of grain-boundary cavities completely within a thick (~1 μm) section of a foil from a simulated welded structure of a pressure vessel steel [18]. The cavities, which are thought to be initiated at grain-boundary discontinuities, are shown in this micrograph to be polyhedral in form. (Micrograph by Kurt Norrgård, Atomenergi, Studsvik, Sweden.)

4. Microanalysis using scanning transmission electron microscopy

4.1. Micro-diffraction

As seen from Fig. 1, by holding the probe stationary it is possible to obtain convergent beam diffraction patterns from areas which are much smaller than those attainable from conventional TEM selected-area diffraction. Selected-area (parallel beam) diffraction is, in principle, only limited by the size of the probe used, although scattering processes in the sample and contamination [13] result in a minimum SAD of ~0.02 μm for a 0.003 μm probe size [8, 9] in a TEM + STEM system, and ~0.01 μm for a correspondingly smaller spot size in a field emission STEM [10, 22]. A more diffuse diffraction pattern may also be obtained by using a very highly convergent beam (see Fig. 1) and this may reduce the ultimate resolution to ~0.005 μm. An example [6] of the excellent micro-diffraction facility in a 200 kV TEM + STEM, compared with conventional TEM selected-area diffraction is shown in Fig. 6a to c. Fig. 6a shows an Al–20 wt% Ag alloy aged to produce a fine continuous dispersion of γ' precipitates of thickness ~10 to 20 nm. As shown in Fig. 6b, a conventional TEM selected-area diffraction pattern is too widespread to exhibit reflections from individual precipitates, showing instead a mixture of reflections from both the matrix and precipitates of different orientations. The micro-diffraction pattern of Fig. 6c, however, reveals reflections from the matrix and a single precipitate. The technique of STEM micro-diffraction has also been applied for example, to the study of very fine crystallites in gold–silver thin film couples [23] and very small carbide particles in steel [24], in both cases of which the volume fraction is so small that individual regions or particles can only contribute weakly to a conventional SAD pattern. By using a small diameter probe, however, very small volume fractions may effectively be increased thereby improving their resolution in diffraction.

Convergent beam diffraction patterns also

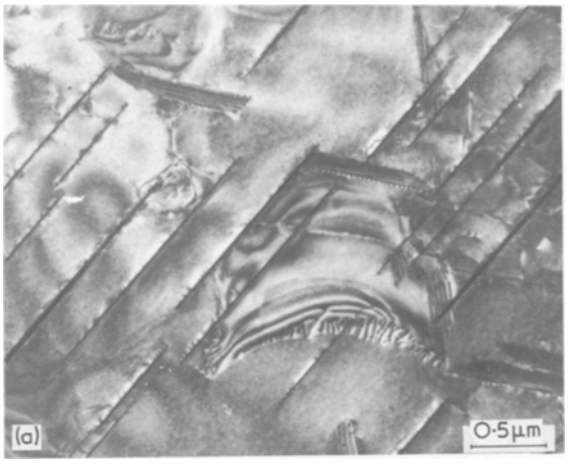

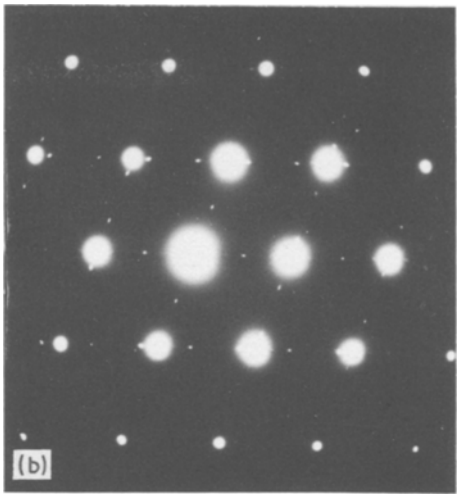

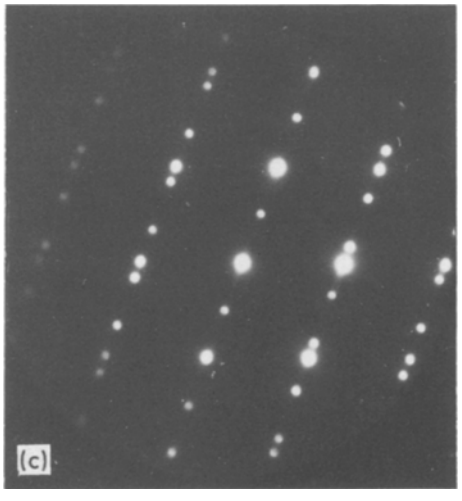

Figure 6 (a) Al–20% Ag alloy, aged 4 h at 320° C to produce γ' silver rich precipitates. (b) Conventional SAD pattern of structure in (a), zone axis: $[1\,1\,0]_{Al}$ // $[1\,1\,\bar{2}\,0]_{ppt}$, showing reflections from several precipitates. (c) Micro-diffraction pattern from a single precipitate (after Bengtsson *et al.* [6]).

afford a convenient way of measuring foil thickness to an accuracy of ± 2% [25]. By employing a two beam condition and using a fairly large convergent beam angle ($\sim 5 \times 10^{-2}$ rad), the spacing of intensity oscillations corresponding to the extinction distance of the material under examination, together with the spacing of the operating reflection can be accurately measured and related directly to the foil thickness. The particular attraction of this technique is that the small area spacial resolution of micro-diffraction allows the thickness measurements to be very accurately positioned on the specimen. The measurement is also independent of the tilt angle of the foil, always giving the actual thickness traversed by the probe.

4.2. Channelling patterns

In principle, the contrast from electron channelling patterns should be improved by using higher brightness guns [26] and this, together with superior lens design, combine to improve the resolution of these patterns when imaging in SEM mode. In a similar way, the contrast from magnetic domain structures can also be improved [27, 28], due evidently to the decreased influence of surface defects on the displayed image when using higher electron velocities. An example of the magnetic domain structure in an Fe–3% Si alloy, as a function of operating voltage between 100 and 200 kV, is shown in Fig. 7a to c. The domain structure in this case was imaged in back-scattered reflection mode using the pair detector and employing the double differentiating mode for recording the image. The specimen was located at the normal position but with the objective lens current switched off. A channelling pattern imaged from the same area as observed in Fig. 7a to c is shown in Fig. 7d, demonstrating once again the impressive versatility of STEM.

5. Chemical analysis based on scanning transmission microscopy

When used in conjunction with an X-ray spectrometer attachment, chemical microanalysis from areas of thin sections, of the order of the size of the probe, can be obtained. In practice, the minimum usable probe diameter is governed by such factors as: the specimen composition and thickness, the incident beam current, the required accuracy of the analysis, specimen drift during X-ray counting, and specimen contamination [6].

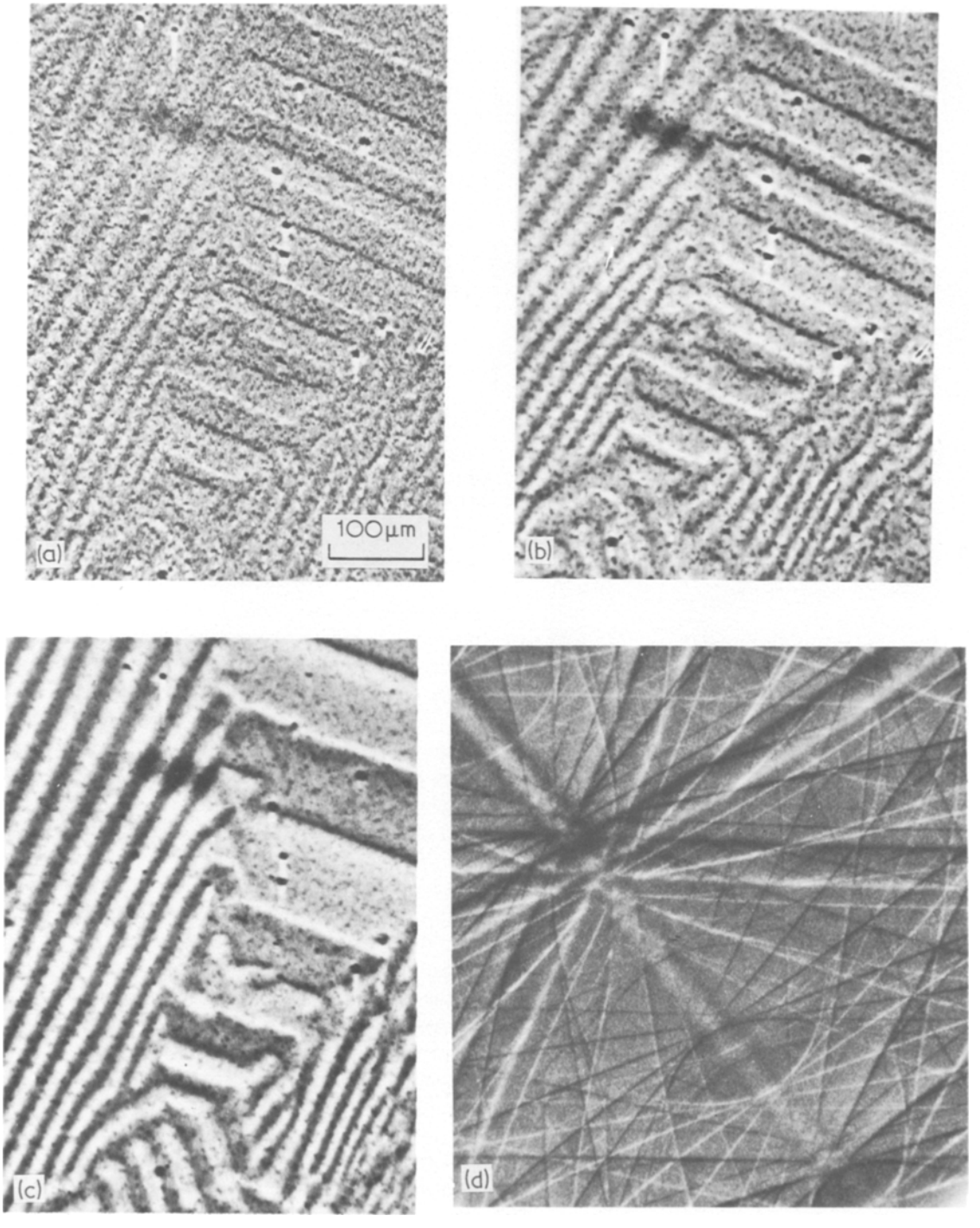

Figure 7 Illustration of the improvement in contrast from magnetic domains in an Fe–3% Si alloy, (a) to (c), when increasing the accelerating voltage up to 200 kV. The specimen was located at the normal position, but with the objective lens switched off. The channelling pattern (d) was imaged from the same area as the micrographs in (a) to (c). Unpublished research by Jakubovics (University of Oxford) and Loberg (University of Luleå). (a) 100 kV, (b) 150 kV, (c) 200 kV.

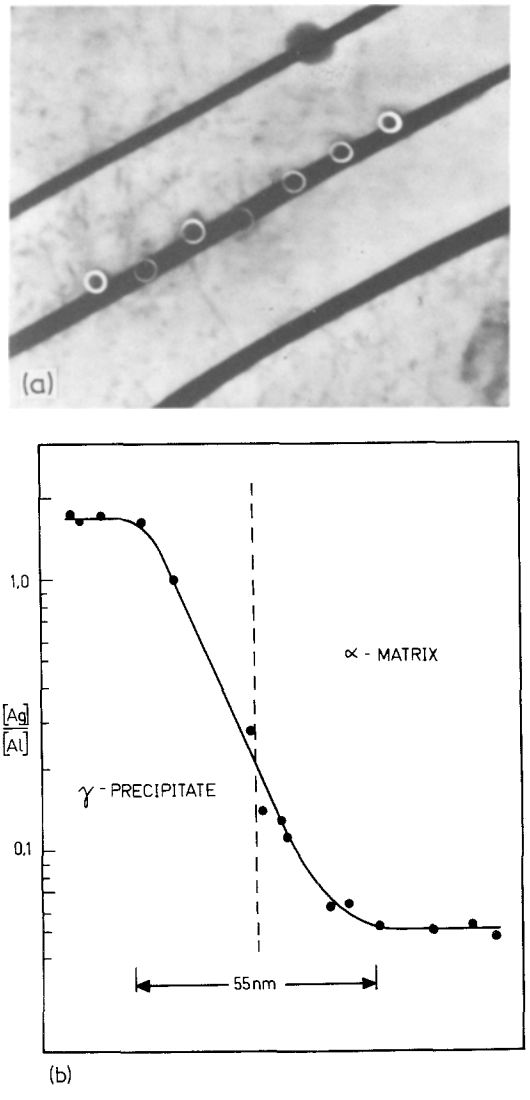

Figure 8 Illustrating the spacial resolution of chemical analysis obtained with a 200 kV STEM + EDX system. (a) Part of a cellular region of an Al–20% Ag alloy tilted to give a vertical interface between the matrix and silver-rich particles. The small rings observed are contamination marks left after the point analyses were made. (b) Plot of the relative intensities of the Ag and Al peaks for the various positions indicated in (a) (after Porter, unpublished research).

Beam currents needed for chemical analysis in thin foils where the volume sampled may be only of the order of $\sim 10^{-17}$ g should be $\gtrsim 10^9$ A. This limits the theoretical resolution of chemical analysis in a 200 kV STEM microscope to ~30 nm [6], although experimentally, contamination and specimen drift tend to increase this value to ~50 nm. In any case, this is still about five times better than the electron microscope microanalyser (EMMA) and some fifty times better than conventional SEM-based X-ray spectroscopy or electron probe microanalysis. Fig. 8b shows a plot demonstrating the spatial resolution of chemical analysis in a 200 kV STEM + EDX system, based on measurements of silver-rich precipitates in an aluminium matrix of the type shown in Fig. 8a. Another example of the technological application of STEM + EDX techniques reported, concerned the study of segregation profiles of Cr, Ni, Mo, S and P in sub-micron wide regions of δ-ferrite in duplex stainless steel weld metals [29].

An elegant example in which STEM + EDX was used in conjunction with micro-diffraction in order to establish the identity of certain precipitates in a complex aluminium alloy is illustrated in Fig. 9. In this case [30], the decomposition of supersaturated Al–Mn alloys containing small amounts of Si and Fe, can result in a variety of precipitate phases. The combined use of micro-diffraction and microanalysis enables these phases to be identified unambiguously. In the example illustrated here, the micro-diffraction pattern indicated, that the precipitate is either a–$Al_{12}Mn_3Si$ or the binary Al–Mn G′ phase. Since both these phases are based on a cubic lattice with $a = 12.5$ to 12.7 Å, it is difficult to distinguish between them by electron diffraction alone. By using energy dispersive analysis, however, it was simple to establish the presence or absence of silicon in the precipitate. In this case the detection of a small amount of silicon confirmed that the precipitate is in fact a–$Al_{12}Mn_3Si$.

There are many advantages in carrying out chemical analysis in thin foils, quite apart from the excellent spacial resolution of the technique. For instance the reduced electron scattering of the probe when traversing thin sections compared to "bulk" analysis, effectively simplifies the absorption and fluorescence corrections needed for quantitative analysis [31]. In addition the low absorption results in more uniform background radiation (bremsstrahlung) thereby facilitating background subtraction for quantitative analysis. A disadvantage of using high probe currents, however, is the relatively high rate of contamination due to the presence of oil vapour in the vicinity of the probe. However, recent work at the University of Oxford has shown that contamination can be reduced practically to zero by heating the sample to ~200° C. The higher vacuum boride gun systems of the future should be less susceptible to contamination. Another problem

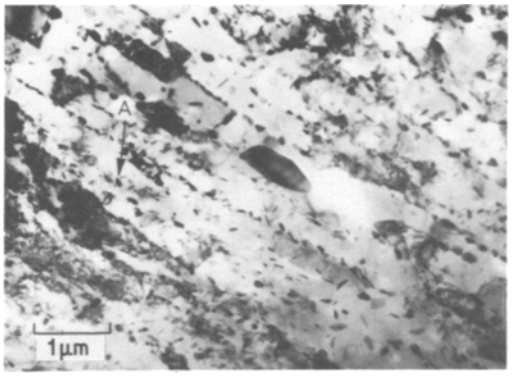

Al - 1·8 wt.% Mn ALLOY – COLD ROLLED AND PARTIALLY ANNEALED FOR 5 min at 500°C

MICRODIFFRACTION PATTERN OF PRECIPITATE (A) THIS PATTERN IS CONSISTENT WITH THE CUBIC α-$Al_{12}Mn_3Si$ STRUCTURE. THE ELECTRON BEAM DIRECTION IS WITHIN A FEW DEGREES OF <100>

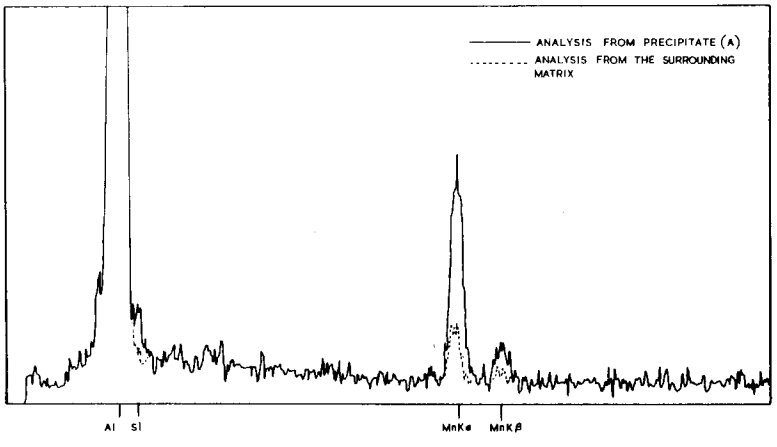

ENERGY DISPERSIVE ANALYSIS OF PRECIPITATE (A) INDICATING THE PRESENCE OF SILICON AND CONFIRMING THAT THE PARTICLE IS α-$Al_{12}Mn_3Si$

Figure 9 The combined use of micro-diffraction and microanalysis for the identification of small precipitates in a complex aluminium alloy (courtesy of Dr. P. L. Morris and Mr M. D. Ball, Alcan International Ltd, Banbury, UK).

which has been reported in connection with thin foil quantitative analysis, is the apparent effect of oxide formation in increasing the level of oxidizing elements at the edges of thin wedge-section foils [30]. All the observations made of this phenomenon, however, have concerned STEM–EDX or EMMA analyses at or below 100 kV. We have not encountered this problem in our work when using a 200 kV probe, and it is possible that the phenomenon is more relevant to lower voltages and very thin sections.

The digitalized form of the displayed image in STEM mode is very suitable for carrying out on-line image analysis (e.g. for measuring volume fraction second phase particles, particle size distributions, mean free paths, particle morphologies, etc, of both transmitted and reflected images in the STEM. Image analysis attachments based on mini-computers are now available for use with SEMs [7], but when they are used with a STEM better resolution and consequently improved image discrimination are to be expected. We have investigated image analysis of particles in STEM mode using a carbon-extraction replica technique. The latter method, in particular, has given very promising results, in that image discrimination and resolution are superior to back-reflected electron images. It is expected that this type of analysis will be a useful complement to existing QTM work based on light microscopy imaging. The feasibility of combining X-ray spectroscopy with image analysis in SEM and

STEM is also currently being investigated in our laboratory and elsewhere [32].

6. Future outlook of scanning transmission microscopy

The superior processing facilities of STEM, coupled with its less complicated lens arrangement compared with conventional transmission microscopy, are likely to result in interesting developments in HVEM + STEM as well as high voltage pure STEMs in the coming years. In the 100 to 200 kV range there will be developments in high brightness emitters, which, together with the higher vacuum requirements of these sources, will result in higher resolution microscopes and improved chemical analysis facilities.

As seen from Fig. 1, there are no image forming lenses below the objective in STEM, and this is important in several respects. To begin with there is a saving of column space and cost, both of which are particularly relevant when considering high voltage instruments [32, 33]. Furthermore, the fact that most of the electron beam is stopped at the entrance aperture of the first demagnifying lens in STEM mode [14] means that the current at the specimen level is several orders of magnitude lower than that of 1000 kV HVEM, so that radiation shielding may be substantially reduced in this case. When studying light elements, a medium voltage STEM would be preferred to HVEM in order to reduce susceptibility to radiation damage. The absence of lenses below the objective also excludes the possibility of chromatic aberration which may be important when studying very thick samples at high resolution. Another likely advantage of HV–STEM compared with conventional HVEM is the improved possibilities offered for *in situ* experiments because of the better image forming facilities available in both STEM and SEM modes. The development of convergent beam and scanning facilities in HVEMs would certainly broaden their application considerably particularly in chemical analysis and micro-diffraction as well as in *in situ* experiments. Preliminary work on ~500 Å spot size convergent beam 1000 kV microscopy by Moodie at the University of Oxford has shown, for instance, that the angular rotation between two adjacent crystals can be measured to an accuracy of about a minute of arc. This derives from the fact that the angular displacent of the diffracted beams by the two crystals is very well defined by the sharp wide-angle reflections in high voltage convergent beam diffraction. Environmental stages could be simplified and improved since there would be no need for a gas-vacuum stage on both sides of the specimen [34], with a corresponding reduction in deterioration of beam intensity.

For metallurgical applications the combined 100 to 200 kV TEM + STEM systems appear to offer the most advantages at present. When the higher vacuum instruments containing boride emitters are developed later, metallurgists may look forward to structural resolutions in STEM and SEM modes comparable to those of present day TEM, to chemical spacial resolutions as low as 20 nm and micro-diffraction of areas less than 10 nm. Judging by the present rate of development of mini-computers, sophisticated on-line image analysis and on-line quantitative chemical analysis of thin foils will shortly be standard practice. In many respects, however, the most important advantage of scanning transmission electron microscopy over conventional electron microscopy is best represented by its greater flexibility. Furthermore, its introduction has happily coincided with substantial recent developments in the fields of energy dispersive X-ray spectroscopy, scanning microscopy and solid state systems, all of which are fundamental to the wider use and application of STEM techniques. Indeed, as far as the applied metallurgist is concerned, it would appear that the advent of scanning transmission electron microscopy truly marks the coming of age of quantitative electron microscopy.

Acknowledgements

I am grateful to my colleagues, Dr Bengt Loberg, Dr Bo Bengtsson, Dr David Porter and Mr Ralph Harrysson, (University of Luleå), as well as to Dr G. R. Booker (University of Oxford) for stimulating discussions in connection with the contents of this article.

References

1. A. V. CREWE, *Q. Rev. Biophys.* 3 (1970) 137.
2. A. V. CREWE, J. WALL, L. M. WELTER, *J. Appl. Phys.* 39 (1968) 5861.
3. A. V. CREWE, M. ISAACSON, D. JOHNSON, *Rev. Sci. Instrum.* 40 (1969) 241.
4. A. V. CREWE and J. WALL, *Optik* 30 (1970) 461.
5. E. ZEITLER and M. G. R. THOMSON, *ibid* 31 (1970) 258; *ibid* 31 (1970) 359.
6. B. BENGTSSON, B. LOBERG, D. A. PORTER, K. E. EASTERLING, in Proceedings of the 6th

European Congress on Electron Microscopy, Israel (1976) p. 450.
7. K. E. EASTERLING, *Int. Metals Rev.* (1977) in press.
8. W. KUYPERS, M. N. THOMPSON, W. H. J. ANDERSON, Proceedings of the 6th SEM Symposium, 1973, edited by O. Johari and I. Corvin (I.I.T. Research Institute, Chicago, 1973) p. 9.
9. H. KOIKE, S. SAKURAI, K. UENO, W. WATANABE, Proceedings of the International Congress on Electron Microscopy, edited by J. V. Sanders and D. J. Goodchild, Vol. 1 Australian Academy of Sciences, Canberra, (1974) p. 48.
10. J. R. BANBURY, *ibid* p. 44.
11. H. AHMED and W. C. NIXON, in [8], p. 217.
12. D. C. JOY, Proceedings Advances in Analysis of Microstructural Features by Electron Beam Techniques, (Metals Society, London, 1974) p. 20.
13. J. M. COWLEY, in [9], p. 18.
14. *Idem, J. Appl. Cryst.* **3** (1970) 49.
15. G. R. BOOKER, D. C. JOY, J. P. SPENCER, H. GROF VON HARRACH, Proceedings of the 7th SEM Symposium, 1974, edited by O. Johari and I. Corvin (I.I.T. Research Institute, Chicago, 1974) p. 225.
16. J. R. SELLER and J. M. COWLEY, in [8], p. 244.
17. T. YAMAMOTO, H. NISHIZAWA, K. SHIBATOMI, in [9], p. 286.
18. H. L. FRASER and I. P. JONES, *Phil. Mag.* **32** (1975) 225.
19. H. L. FRASER, I. P. JONES, M. LORETTO, private communication (1976).
20. M. H. LORETTO and R. E. SMALLMAN, "Defect Analysis in Electron Microscopy" (Chapman and Hall, London 1975) p. 105.
21. L-G. LILJESTRAND, M. AACOUTUTIER, P. LINDHAGEN, G. ÖSTBERG, I. I. W. DOC. "The formation of microcracks during stress relief annealing of a weldment of the pressure vessel steel A508 C12", (1976).
22. D. C. JOY, H. VON HARRACH, G. E. VERNEY, G. R. BOOKER, in [9], p. 46.
23. S. K. KLANG and I. M. BERNSTEIN, Phil. Mag., to be published.
24. D. A. PORTER and G. DUNLOP, in [6], p. 570.
25. P. M. KELLY, A. JOSTSONS, R. G. BLAKE, J. P. NAPIER, *Phys. Stat. Sol. (a)* **31** (1975) 771; P. M. KELLY, *ibid* **32** (1975) 529.
26. G. R. BOOKER, D. C. JOY, J. P. SPENCER, C. J. HUMPHRIES, in [8], p. 251.
27. T. YAMAMOTO, H. NISHIZAWA, K. TSUNO, *J. Phys. D: Appl. Phys.* 8 (1975) L 113.
28. T. YAMAMOTO, H. NISHIZAWA, K. TSUNO, *Phil. Mag.* **34** (1976) 311.
29. H. ÅSTRÖM, B. LOBERG, B. BENGTSSON, K. E. EASTERLING, *Metal Sci. J.* **10** (1976) 225.
30. D. P. L. MORRIS and M. D. BALL, Alcan International Ltd, Banbury (1976) unpublished research.
31. H. YAKOWITZ, in [12], p. 1029.
32. S. EKELUND, Institute of Metals Research, Rep. No. IM 1103, Stockholm (1975).
33. E. ZEITLER and A. V. CREWE, in [9], p. 40.
34. J. M. COWLEY, "Physical aspects of electron microscopy and microbeam analysis", edited by B. M. Siegel and D. R. Beaman (Wiley, New York, 1975) p. 17.

Received 13 April and accepted 6 September 1976.